Supporting Information

Jeffrey *et al.* 10.1073/pnas.0711232105

SI Text

Reagents. Reagents were from Sigma unless otherwise indicated. The following drugs were used: 10 μM nifedipine, 25 μM E64D, 100 μM diazoxide, 1 μM thapsigargin, and 100 μM ALLM (Calbiochem). Palmitic acid (Nu-Check Prep N-16-A) was dissolved in 65 mM NaOH and complexed with 20% essentially fatty acid-free BSA (Sigma). The complex was added to DMEM media or RPMI 1640 media containing 10% FBS and 2% penicillin–streptomycin for a final molar ratio of 6:1 palmitate (1.5 mM) to BSA, unless otherwise indicated. A vehicle control was included for each experiment.

Animals. CPE$^{fat/fat}$ mice on the C57BL/6J background and littermate controls were obtained from The Jackson Laboratories. Intraperitoneal glucose tolerance tests (IPGTT; 2 g of glucose per kg of body weight) were performed on males after a 12-h fast. In some studies, male C57BL/6J mice were fed a high-fat diet (40% of calories from fat, TD88137; Harlan Teklad) for 6 months and compared to littermate controls fed normal chow. During this period, mice fed normal chow grew in weight from 22.4 $\pm$ 0.4 g to 33.1 $\pm$ 0.7 g, whereas mice fed high fat grew from 22.2 $\pm$ 0.3 g to 42.7 $\pm$ 1.2 g ($P > 0.05$). Fasting blood sugars in chow-fed mice increased modestly (5.4 $\pm$ 0.2 to 6.5 $\pm$ 0.7), whereas high-fat-fed mice showed a robust increase in 12-h fasting glucose (6.0 $\pm$ 0.3 to 9.5 $\pm$ 0.5). All studies were approved by the University of British Columbia Animal Care Committee in accordance with national guidelines.

Cell Culture. Human islets were provided by either the Washington University Islet Transplantation Center or the Centre for Human Islet Transplant and β-cell Regeneration at the University of British Columbia and cultured as described (1–3). Our protocol (4) for isolating islets from male 3- to 4-month-old C57BL/6J mice is a technique modified from the original described by Lacy and Kostianovsky (5), with a filtration step adapted from Salvalaggio *et al.* (6). MIN6 cells were cultured in DMEM (GIBCO/Invitrogen) with 10% FCS, antibiotics, and 25 mM glucose unless otherwise indicated. Hormone release or hormone contents from MIN6 cells and human islets was assessed by static incubation or perfusion, as described (7). Insulin and proinsulin were assayed with Linco RIA or ELISA, respectively.

Immunofluorescent Staining. MIN6 cells plated onto polylysine-coated coverslips were fixed in fresh 4% paraformaldehyde for 10 min, permeabilized with Triton X-100 for 10 min, and blocked with goat serum. CPE was detected by using a monoclonal primary antibody (BD Biosciences) and goat secondary antibody conjugated to FITC (Jackson ImmunoResearch). Primary antibodies to insulin (Linco) or the Golgi marker GM130 (BD Transduction Laboratories) were detected with goat secondary antibodies conjugated to Texas red (Jackson ImmunoResearch). Lysotracker red (70 nM; Molecular Probes) was loaded into cells at 37°C for 30 min. Unless otherwise indicated, β-cell area and α-cell area were stained using guinea pig anti-insulin antibody and rabbit anti-glucagon antibody (Linco/Millipore). Proliferation was measured with anti-PCNA. CPE-cleaved mature insulin was detected with a monoclonal antibody, clone mAB1, from Biodesign/Meridian. Cells and pancreas sections were mounted in Vectashield solution with DAPI, and imaged by using a Ziess $\times$100 (1.45 numerical aperture) objective, individual filter cubes for each color (Roper Scientific), and a CoolSnap HQ2 Camera. Images were deconvolved by using Slidebook software (Intelligent Imaging Innovations). Staining of paraffin-embedded pancreas sections was performed by using standard methods.

Cell Death and Apoptosis Assays. For online, high-throughput imaging of cell death, cells were plated onto clear-bottom 96-well microplates (ViewPlate-96; PerkinElmer) and treated as indicated. The incorporation of propidium iodide (500 ng/ml added to wells) was monitored in the incubated chamber (37°C, 5% CO_2) of a KineticScan Reader (Cellomics). Propidium iodide is a dye that is normally nonfluorescent but fluoresces brightly once it passes through the compromised plasma membrane of dying cells and binds to DNA. Two to four nonoverlapping images were taken from each well at 30-min intervals. The total number of propidium iodide positive cells was then counted from these two images using the Target Activation Bioapplication (Cellomics). The TUNEL assay (Roche) was performed according to the manufacturer's instructions on pancreas sections counterstained with DAPI and anti-insulin antibody (Linco/Millipore).

Proteomic Analysis of MIN6 Cell and Human Islets. Our methods for 2D-DIGE proteomics of human islets have been described (7). Briefly, lysates from control and palmitate-treated cells were labeled with fluorescently distinct Cy dyes and analyzed in the same 2D gel. The Typhoon 9400 imager (Amersham Biosciences) and Decyder-DIA software (Amersham Biosciences) were used to quanitfy individual spots, which were considered significantly different if they were >2 standard deviations outside of the normalized distribution of gel feature intensities, corresponding to a ≈1.4-fold change in volume ratio for these images. Significantly different spots were manually selected, using fold-change and resolution criteria, for sequencing by using either MALDI-TOF/TOF (Proteomics 4700; Applied Biosystems) or LC-MS/MS (Q-STAR XL; Applied Biosystems), under the conditions previously described (8).

Immunoblot. Cells were washed with PBS and detached in the presence of 100 μl lysis buffer with PMSF. Cells were further lysed through sonication. Fifteen to 35 μg of protein was separated in 12% SDS/PAGE gels and transferred onto PVDF membranes by using semidry transfer (BioRad). These membranes were incubated with I-Block (Applied Biosystems) with 0.1% Tween 20 (Sigma) for 1 h. Membranes were incubated with primary antibodies for either 2 h at 18°C or overnight at 4°C. Rabbit monoclonal antibody to cleaved caspase-3 was from Cell Signaling Technologyzcomx. Rabbit polyclonal anti-CHOP antibody was from Santa Cruz Biotechnology. Unless otherwise indicated, all CPE blots used an antibody that targets the zinc-binding region of the protein (BD Biosciences). Polyclonal antibodies to the N and C termini of CPE were from Serotech and Chemicon, respectively. Carboxypeptidase D antibody was a gift from Catherine Too (Dalhousie University, Halifax, Canada). Antibodies to prohormone convertase-1/3 and prohormone convertase-2 were from Chemicon.

shRNA-Mediated CPE Knockdown and CPE Overexpression. CPE levels were reduced in MIN6 cells using a vector expressing shRNA sequences designed against CPE (GGT GGA ATG CAA GAC TTC AAT) from SuperArray. A scrambled shRNA sequence (GGA ATC TCA TTC GAT GCA TAC) purchased from SuperArray and GFP were used as controls. Plasmid DNA (2 μg)

was transfected using Lipofectamine 2000 (Invitrogen), resulting in GFP expression in ≈20% of cells after 40 h. GFP-positive cells were sorted by fluorescence-activated cell sorting (BD FACS Vantage SE/DIVA).

CPE was transiently overexpressed in MIN6 cells. CPE plasmids, one under the control of the CMV promoter and another under the control of the rat insulin promoter, were kindly supplied by L. D. Fricker. CPE DNA (1 μg), or empty pcDNA3.1 vector, was transfected into MIN6 cells by using Lipofectamine 2000 (Invitrogen).

1. Johnson JD, *et al.* (2003) Increased islet apoptosis in Pdx1+/− mice. *J Clin Invest* 111:1147–1160.
2. Johnson JD, Misler S (2002) Nicotinic acid-adenine dinucleotide phosphate-sensitive calcium stores initiate insulin signaling in human beta cells. *Proc Natl Acad Sci USA* 99:14566–14571.
3. Johnson JD, *et al.* (2004) RyR2 and calpain-10 delineate a novel apoptosis pathway in pancreatic islets. *J Biol Chem* 279:24794–24802.
4. Lacy PE, Kostianovsky M (1967) Method for the isolation of intact islets of Langerhans from the rat pancreas. *Diabetes* 16:35–39.
5. Salvalaggio PR, *et al.* (2002) Islet filtration: a simple and rapid new purification procedure. *Transplantation* 74:877–879.
6. Luciani DS., Johnson JD (2005) Acute effects of insulin on beta-cells from transplantable human islets. *Mol Cell Endocrinol* 241:88–98.
7. Johnson JD, *et al.* (2006) Insulin protects islets from apoptosis via Pdx1 and specific changes in the human islet proteome. *Proc Natl Acad Sci USA* 103:19575–19580.
8. Bredemeyer AJ, *et al.* (2004) A proteomic approach for the discovery of protease substrates. *Proc Natl Acad Sci USA* 101:11785–11790.

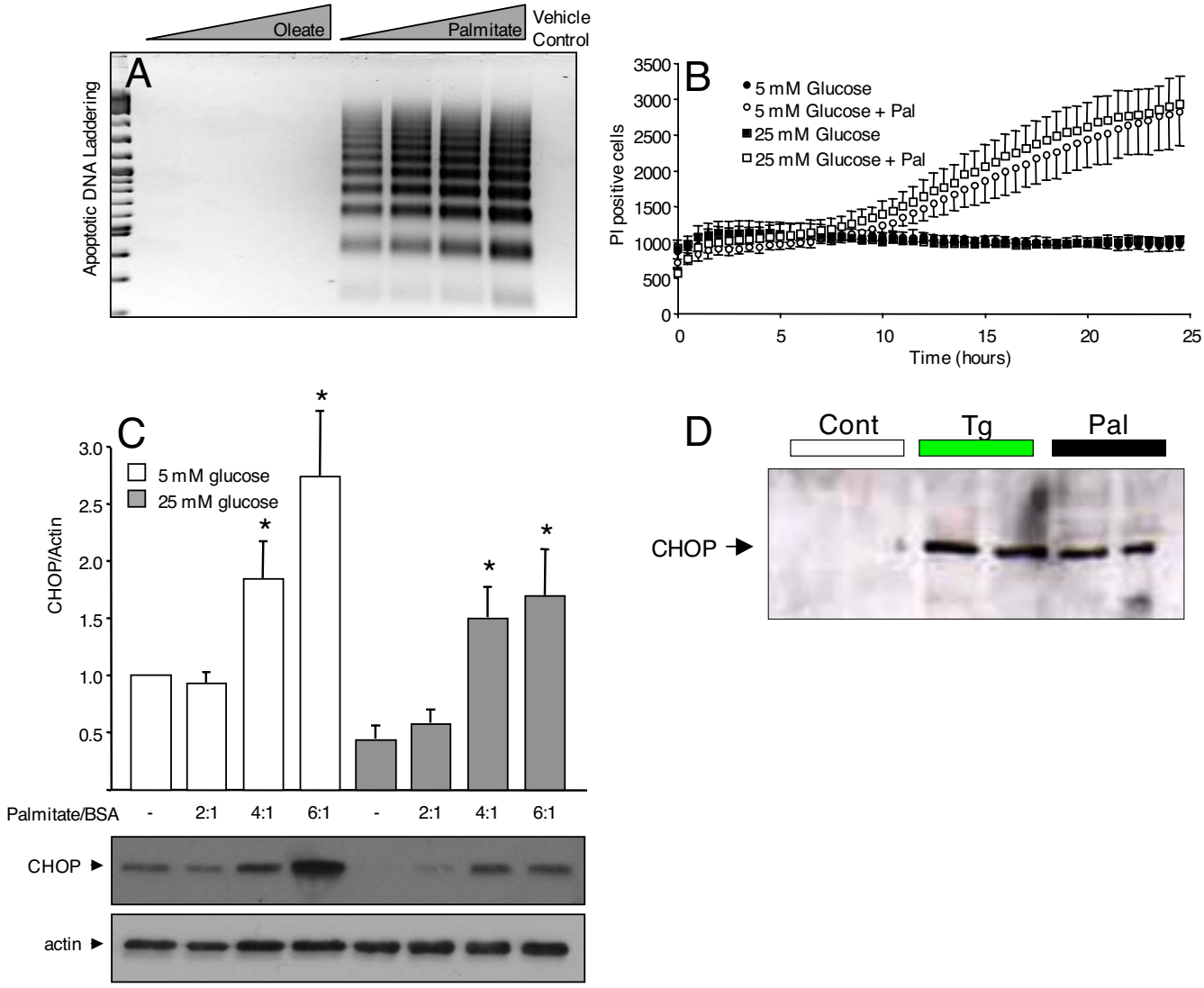

Fig. S1. Characteristics of lipotoxicity in β cells. (*A*) MIN6 cells treated for 24 h with increasing concentrations (100 μM, 250 μM, 500 μM, 1000 μM) of palmitate, but not oleate, show DNA laddering ($n = 3$). (*B*) Real-time monitoring of propidium iodide incorporation in populations of MIN6 cells during exposure to 6:1 palmitate-to-BSA ratio in culture ($n = 3$). (*C*) Dose-dependent increase in ER-stress in MIN6 cells treated with 2:1, 4:1, or 6:1 palmitate-to-BSA ratio for 24 h ($n = 6$). The asterisk denotes significant difference from vehicle-treated controls. (*D*) Palmitate increases CHOP protein in human islets treated for 24 h at 5 mM glucose. Thapsigargin was included as a positive control ($n = 4$).

Carboxypeptidase E: Spot 1650

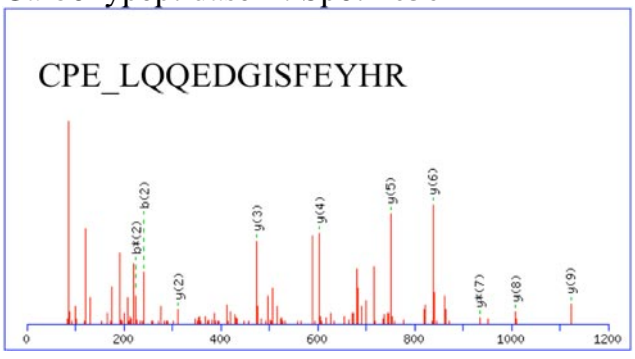

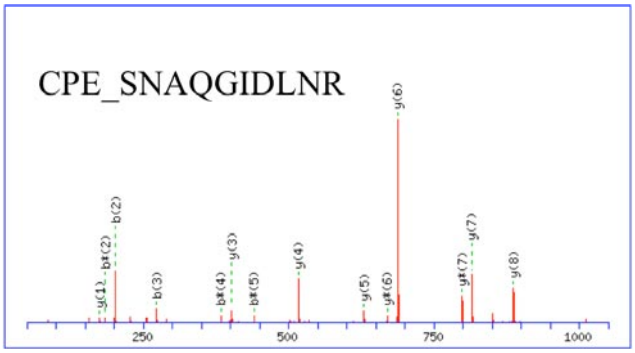

Carboxypeptidase E: Spot 1651

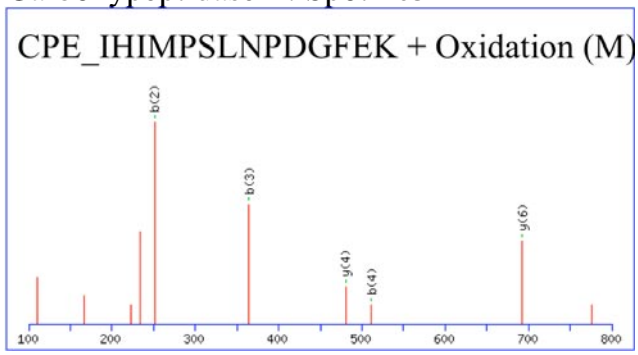

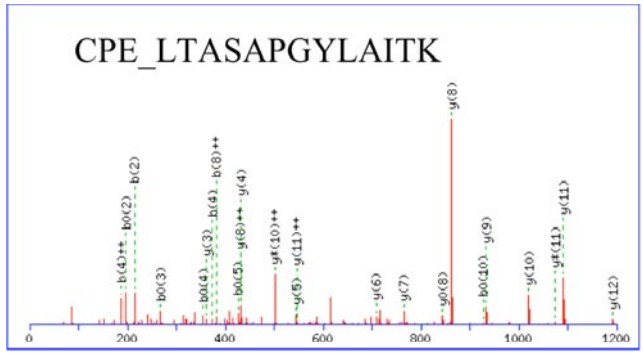

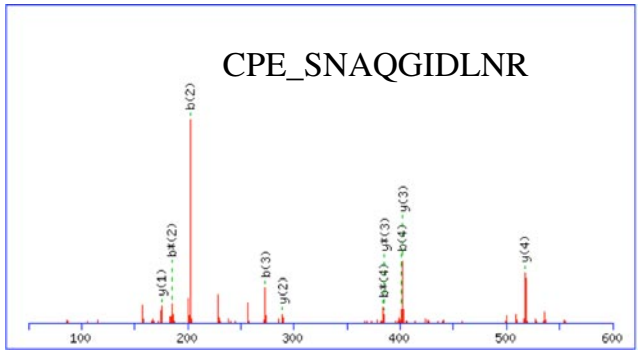

Fig. S2. Proteomic identification of CPE. Tandem mass spectra of mouse CPE peptides found in palmitate-treated MIN6 cells are shown. CPE was identified in two separate spots (1650, 1651). The spectra were acquired on a MALDI-TOF/TOF instrument as previously described (8).

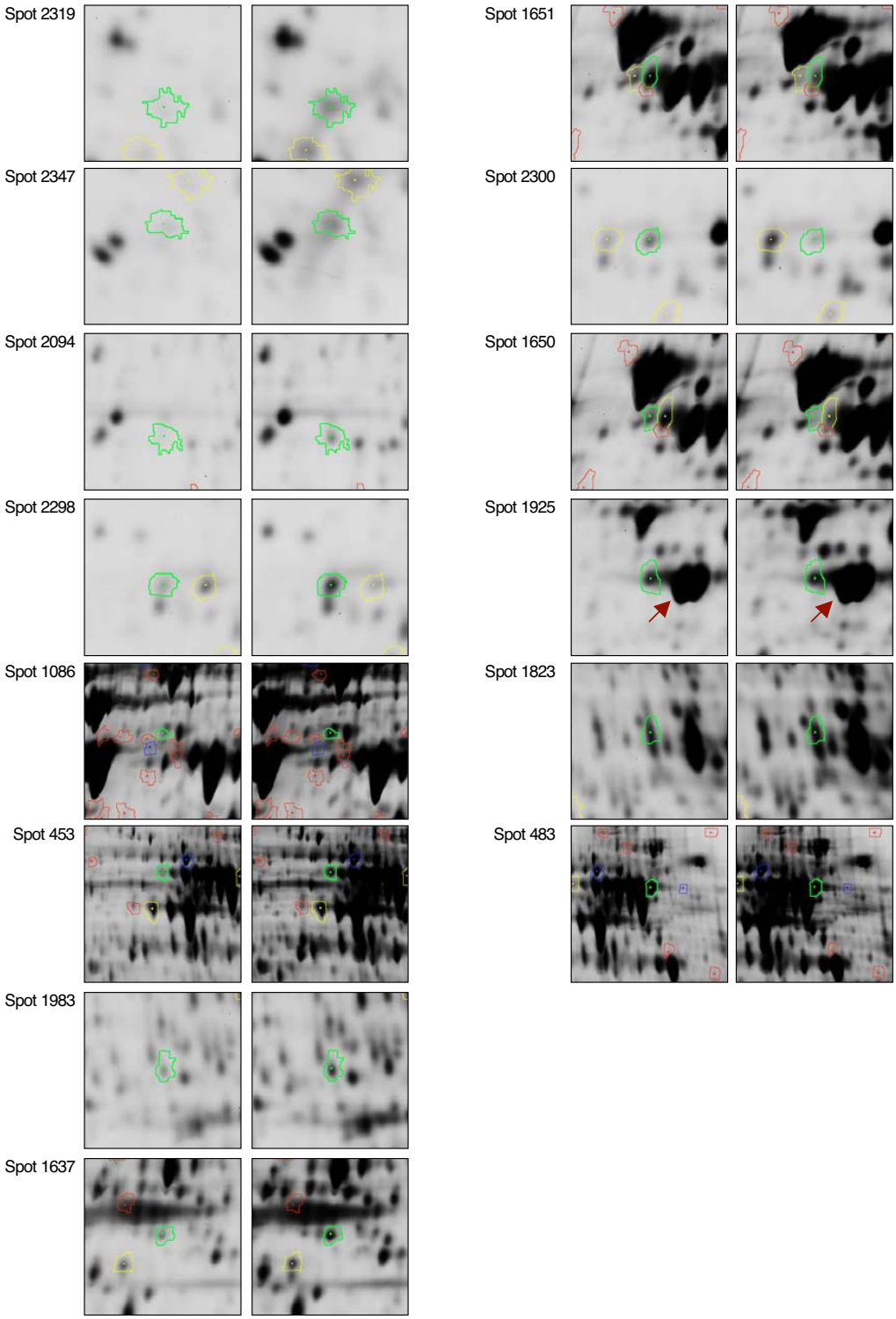

Fig. S3. Gel image detail of features that contained significantly different normalized spot volumes. Raw images of gel features that were significantly increased (*Left*) or decreased (*Right*) in palmitate-treated MIN6 cells are shown as volume plots. See Table S1 for protein identifications. For each image, the identified spot is circled in green. Yellow denotes other identified spots nearby. Note that a single gene product may exist as multiple spots on a 2D protein gel. For example, we detected a spot identified as actin (spot 1925) that appears to be a minor isoform. The large (saturated) spot next to the identified spot is likely to be the major isoform of actin (arrow).

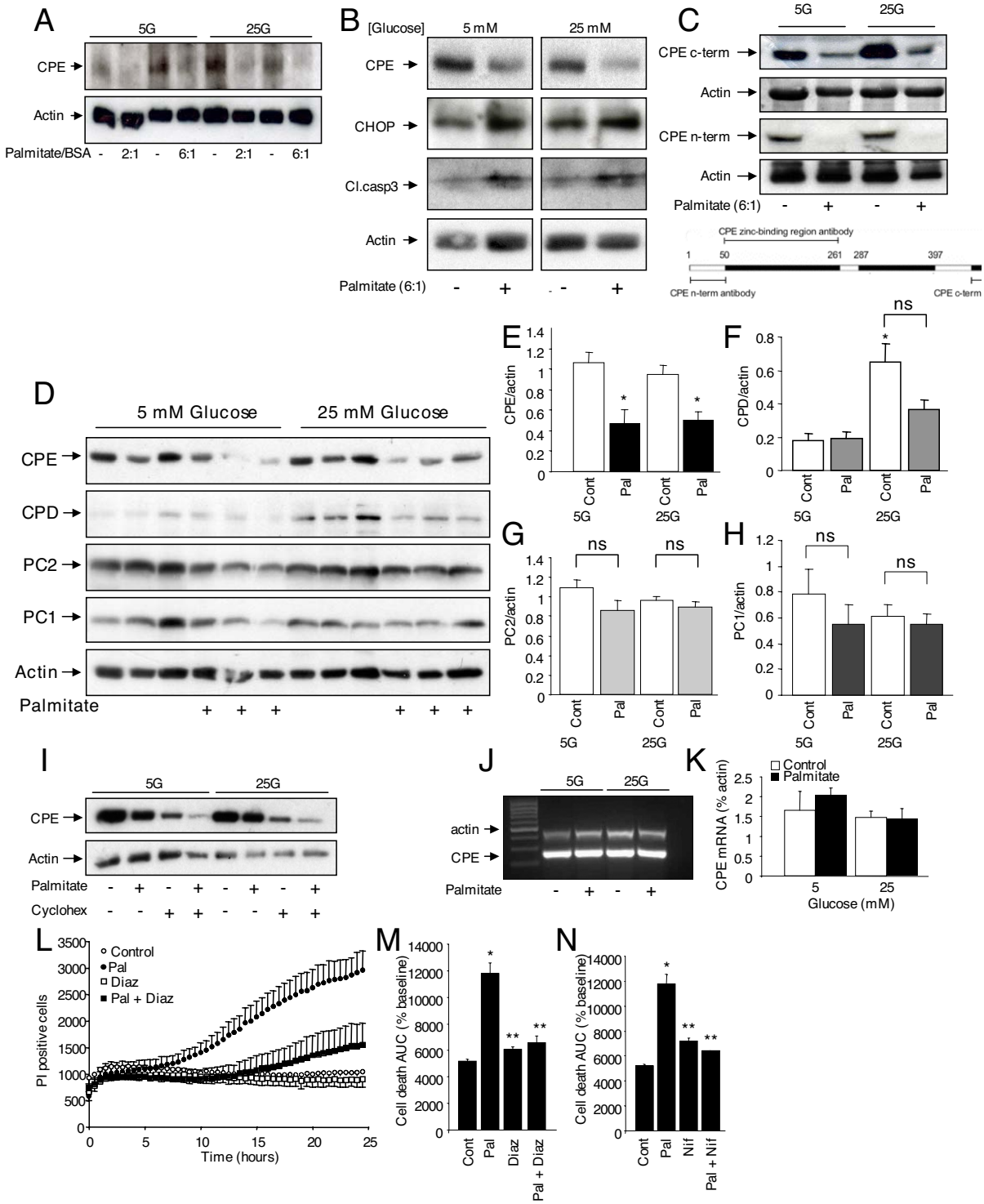

Fig. S4. Palmitate targets CPE specifically relative to other hormone processing enzymes. (*A*) Human islets treated for 48 h with two palmitate:BSA ratios (n = 3). (*B*) Effects of 24-h palmitate treatment (6:1) on CPE, CHOP, and cleaved caspase-3 at both low and high glucose in human islets (n = 3). (*C*) MIN6 cells treated for 24 h with 6:1 palmitate showed a decrease in CPE using C-terminal or N-terminal targeted antibodies. (*D–H*) Effects of 24-hour incubations of palmitate and glucose on prohormone converase 2 (PC2), prohormone converase 1/3 (PC1), and carboxypeptidase D. The asterisk denotes significant difference from 5 mM glucose control. (*I*) MIN6 cells treated with palmitate and/or 10 μM cycloheximide for 24 h (n = 3). (*J* and *K*) No differences in CPE gene expression in MIN6 cells treated with palmitate for 24 h at either low or high glucose were observed with RT-PCR (n = 3). (*G–K*) Effects of 24-h incubations of palmitate and glucose on prohormone converase 2 (PC2), prohormone converase 1/3 (PC1) and carboxypeptidase D. The asterisk denotes significant difference from 5G control. (*L* and *M*) Propidium iodide incorporation in MIN6 cells at 25 mM glucose with palmitate and 100 μM diazoxide (n = 3). (*N*) Quantification of propidium iodide incorporation in MIN6 cells at 25 mM glucose with palmitate and 10 μM nifedipine (n = 3).

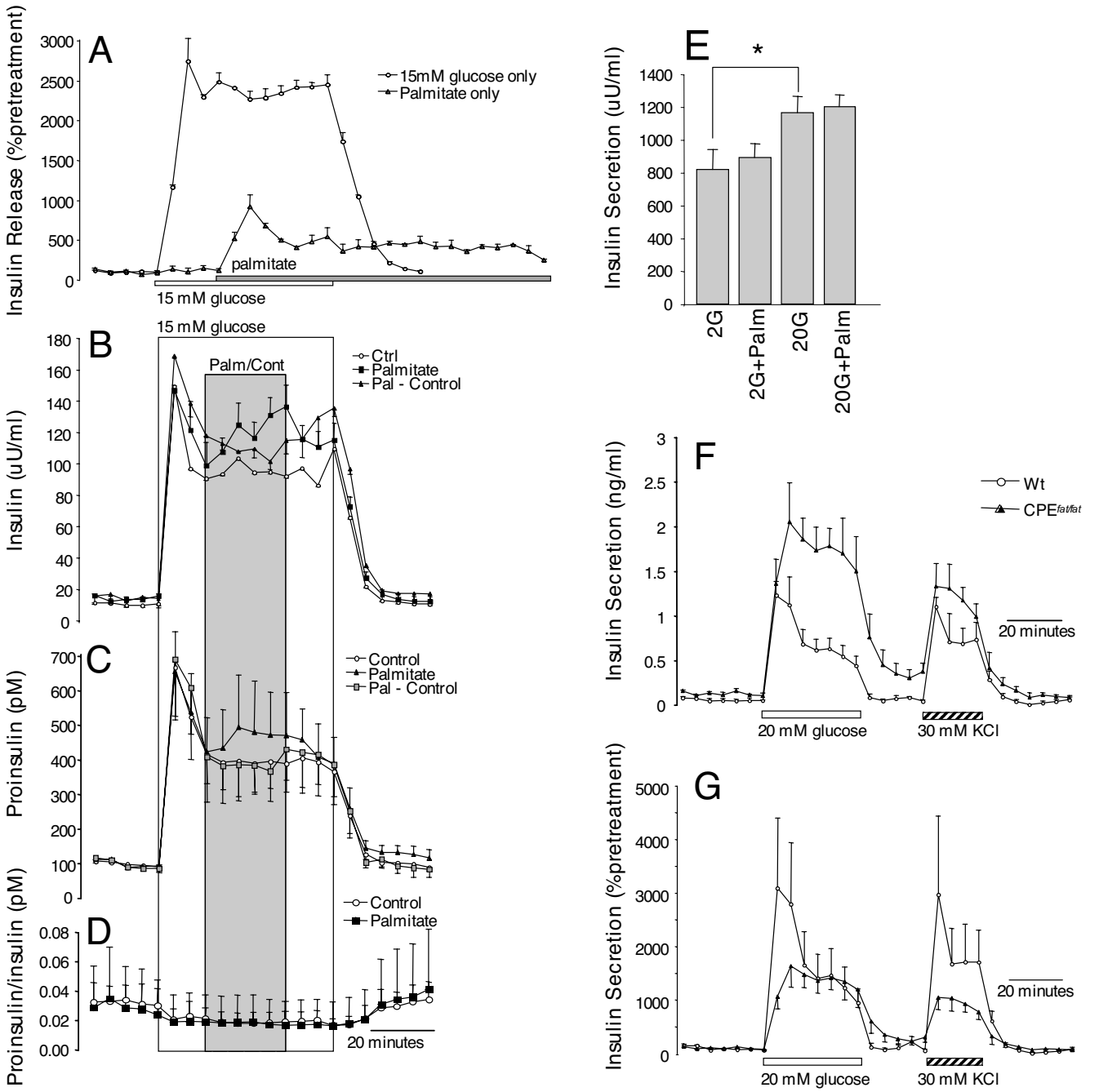

Fig. 55. Acute effects of palmitate and glucose on insulin and proinsulin secretion. (*A*) Groups of 500–1,000 human islets were perifused with Krebs buffer containing 3 mM glucose. The white bar indicates a period when islets (white circles) were exposed to 15 mM glucose. The gray bar indicates a period when islets (gray triangles) were exposed to palmitate. Values are normalized to the pretreatment levels of insulin secretion to control for uneven numbers of islets in each column ($n = 4$). (*B*) Insulin secretion. (*C*) Intact proinsulin secretion. (*D*) The ratio between secreted intact proinsulin and insulin are shown in human islets treated with 15 mM glucose alone (white circles) or 15 mM glucose plus palmitate (black symbols). Some islets were exposed to a vehicle control during glucose stimulation (pal control; gray symbols). ($n = 4–8$). (*E*) Insulin secretion from the same experiments shown in Fig. 3*D*. (*F* and *G*) Dynamics of insulin release from islets isolated from 12-week-old CPE$^{fat/fat}$ mice. Results are shown as raw data and normalized to the pretreatment mean to control for possible basal hypersecretion or the uneven loading of the larger CPE$^{fat/fat}$ islets. Note that there may be some detection of mouse pro-insulin because of the characteristics of the assay.

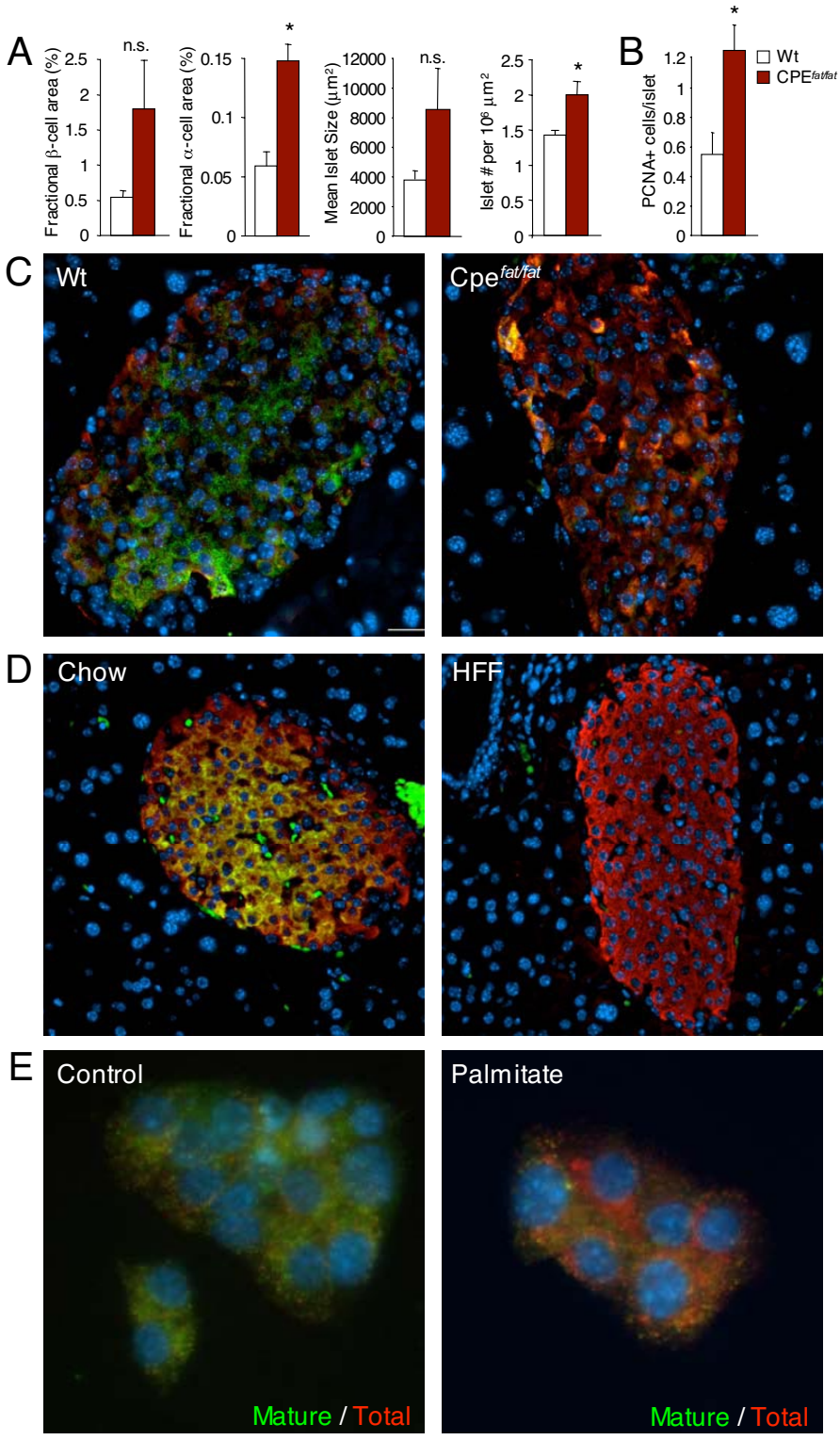

Fig. S6. Altered morphology and insulin maturation in CPE null and high-fat-treated islet cells. (*A*) Fractional β-cell and α-cell area, average islet size (including single cells), and average number of islets (per 1,000,000 μm^2 pancreas area) were measured in pancreas sections from 3-month-old CPE$^{fat/fat}$ mice and compared with wild-type littermate controls ($n = 3$). (*B*) PCNA-positive cells were quantified as an index of β-cell proliferation ($n = 3$). (*C*) The ratio of mature insulin (i.e., CPE cleaved; green) to total insulin (uncleaved and cleaved; red) was substantially decreased in CPE null mice ($n = 3$). (*D*) The ratio of mature insulin (green) to total insulin (red) was substantially decreased in high-fat-fed mice ($n = 3$). (*E*) The ratio of mature insulin (green) to total insulin (red) was substantially decreased in MIN6 cells treated with 6:1 palmitate for 24 h and imaged with a ×100, 1.45NA objective ($n = 3$). Note that all pairs of images were acquired with the same exposure and thresholded with the same intensity values.

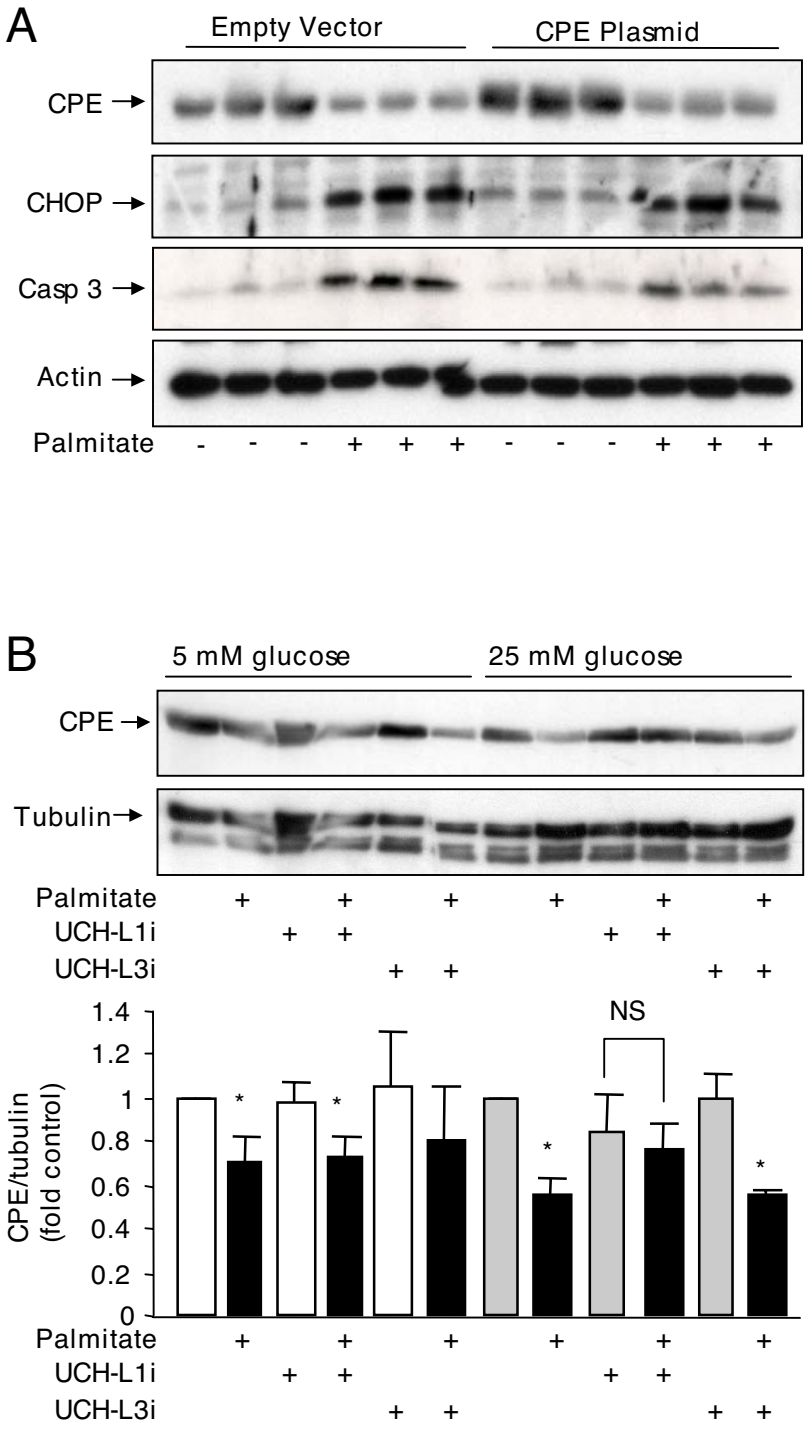

Fig. S7. The effect of UCH-L1 or UCH-L3 inhibitors on palmitate-treated MIN6 cells. (*A*) Raw Western blot image for CPE overexpression data quantified in Fig. 4 *L–N*. (*B*) MIN6 cells were treated for 24 h with palmitate (Pal) and inhibitors for either UCH-L1 (10 μM) or UCH-L3 (50 μM), and the resulting Western blots were quantified ($n = 3$).

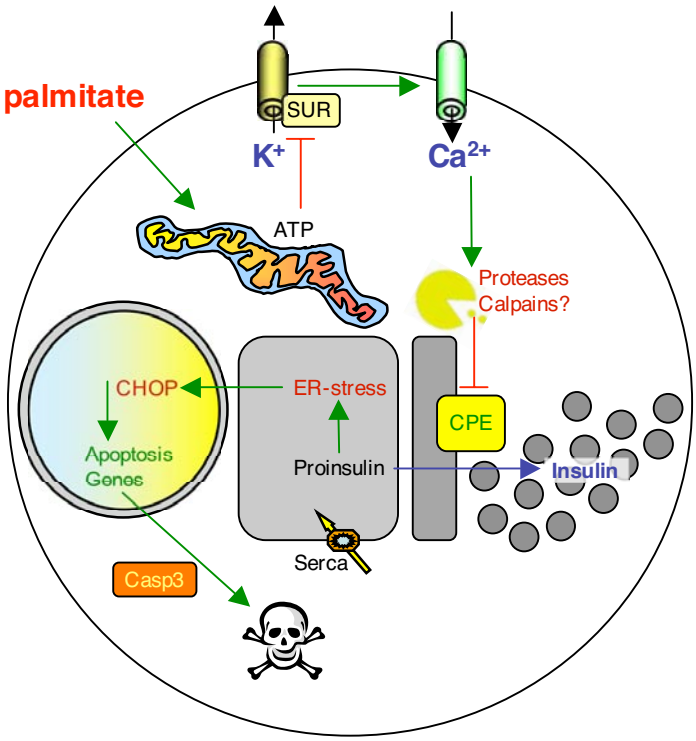

Fig. S8. Schematic working model of palmitate-induced ER-stress and β-cell apoptosis. In this model, palmitate is metabolized to generate ATP, which closes diazoxide-sensitive K_{ATP} channels. This in turn opens nifedipine-sensitive voltage-gate Ca^{2+} channels. The resulting Ca^{2+} influx participates in the degradation of CPE, possibly via the activation of a Ca^{2+}-sensitive protease (e.g., calpain). The rapid loss of CPE impairs the β-cell's ability to process proinsulin, and the accumulation of unprocessed proinsulin might be expected to cause ER stress. The ER stress signals through CHOP to activate programmed cell death.

Table S1. Mass-spectrometry-based identification of differentially expressed spots in palmitate-treated MIN6 cells

Spot no.	Protein	GI code	Fold	Function
Significantly increased				
2319	Ubiquitin carboxy-terminal hydrolase L1	6755929	2.57	Protein degradation, apoptosis, Parkinson's
2347	NADH dehydrogenase Fe-S protein 8	4505371	2.47	Metabolism
2094	Phosphoprotein phosphatase 1-gamma Catalytic chain	109652	2.02	Signal transduction, studied in NIDDM muscle
2094	Nucleoporin 37	21312212	2.02	Nuclear pore complex, mitosis
2298	Proteosome alpha subunit 3	3914438	1.69	Protein degradation
2298	Phosphoglycerate mutase	12844989	1.69	Glycolytic and gluconeogenic pathways
1086	NADH dehydrogenase Fe-S protein 1	27807355	1.68	Mitochondrial, increased in diabetic kidneys
1086	Guanine nucleotide regulatory protein	3461880	1.68	Cell cycle
453	ATP citrate lyase	8392839	1.46	Makes acetyl-CoA for lipid synthesis
1983	40-kDa protein kinase	23879	1.46	MAP kinase isoform
1983	GDP-d mannose-4,6-dehydratase	3258631	1.46	Trafficking
1637	Kappa B motif-binding phosphoprotein	1083569	1.44	Signal transduction
Significantly decreased				
1651	Carboxypeptidase E	115893	−3.64	Proinsulin processing, diabetes, obesity
2300	Phosphoglycerate mutase	12844989	−2.87	Glycolytic and gluconeogenic pathways
2300	Proteosome alpha subunit 3	3814438	−2.87	Protein degradation
1650	Carboxypeptidase E	109628	−2.85	Proinsulin processing, diabetes, obesity
1925	Actin (fragment)	71620	−1.50	Cytoskeleton
1823	DNAJ (Hsp40) homolog, subfamily A, member 1	6680297	−1.34	Motorneuron degeneration
483	ATP citrate lyase	8392839	−1.32	Makes acetyl-CoA for lipid synthesis

Table S2. Mass spectrometry-based identification of differentially expressed spots in palmitate-treated human islets

Spot no.	Protein	GI code	Fold	Function
Significantly increased				
3818	Glucagon	121481	1.68	Islet hormone, glucose homeostasis
527	Protein disulfide isomerase, pancreatic	5803119	1.58	Chaperone
825	DNAK-type molecular chaperone HSP70	483005	1.55	Chaperone
740	α-2-hs-glycoprotein	27806751	1.47	Endocytosis, brain and bone development, apoptosis
2891	Histone H4	11121217	1.42	Chromatin structure
2694	Histone H2B	70716	1.37	Chromatin structure
2697	Histone H2B	70716	1.34	Chromatin structure
Significantly decreased				
1112	Carboxypeptidase E	4503009	−2.11	Proinsulin processing, diabetes, obesity
3378	GC31613	34876364	−1.82	Chromatin structure?
1662	*N*-acetylneuraminic adic phosphate synthase	12056473	−1.59	Sialic acid synthesis
2924	Prosaposin	11386147	−1.46	Lipid binding and presentation in lysosomes
3390	Histone H2B-613	27693390	−1.39	Chromatin structure